Dissipative solitons for generalizations of the cubic complex Ginzburg-Landau equation

M. I. Carvalho*
DEEC/FEUP and INESC TEC, Universidade do Porto, Rua Dr. Roberto Frias, 4200-465 Porto, Portugal

M. Facão†
Departamento de Física, Universidade de Aveiro and I3N Campus Universitário de Santiago, 3810-193 Aveiro, Portugal

(Received 3 May 2019; published 26 September 2019)

We found stable soliton solutions for two generalizations of the cubic complex Ginzburg-Landau equation, namely, one that includes the term that, in optics, represents a delayed response of the nonlinear gain and the other including the self-steepening term, also in the optical context. These solutions do not require the presence of the delayed response of the nonlinear refractive index, such that, they exist regardless of the term previously considered essential for stabilization. The existence of these solitons was predicted by a perturbation approach, and then confirmed by solving the ordinary differential equations, resulting from a similarity reduction, and also by applying a linear stability analysis. We found that these solitons exist for a large region of the parameter space and possess very asymmetric amplitude profiles as well as a complicated chirp characteristic.

DOI: 10.1103/PhysRevE.100.032222

I. INTRODUCTION

Dissipative solitons are a class of localized solutions of nonconservative nonlinear evolution equations that preserve their form as they propagate. The name was coined after the conservative solitons since they share with them the nonlinear character and the undistorted propagation. The dissipative solitons exist due to two types of balances, one between dispersion and a conservative nonlinear effect and the other between linear or nonlinear loss and amplification. The characteristics of the dissipative solitons are determined by the parameters of the evolution equation such that they do not exist as families of solutions as in the case of conservative solutions [1]. They have been theoretically predicted and experimentally observed in several areas, from different branches of physics to biology [2].

Among the evolution equations that admit dissipative solutions, the complex Ginzburg-Landau equation (CGLE) is one that has been studied in different kinds of physical systems, especially because it describes the amplitude evolution of unstable modes close to a Hopf bifurcation [3–5]. In optics, it describes the evolution of the envelope of a wave packet on a medium modeled by linear dispersion up to second order, nonlinear refractive index, linear loss dispersion, linear and nonlinear gain or loss, and saturation of nonlinear refractive index and gain [6–9]. In this latter context, solitons have been observed experimentally [10–12]. In certain cases, the model should also include higher-order effects such as the ones named as gradient terms [5,13,14] that, in optics, correspond to delayed response and dispersion of the nonlinear refractive index and nonlinear gain.

The CGLE equation and its generalizations, including the higher order effects referred above, have been known to admit solitons in specific regions of its parameter space, but not all the solitons are stable, such that we have regions of existence and smaller regions of stable solitons. In the particular case of the cubic CGLE, the solitons are stable in a parameter region where the background state is unstable, due to the existence of linear gain; thus noise will be amplified and will eventually perturb the soliton [15]. However, if the gradient terms are added to the cubic CGLE, one usually observes the onset of a new localized solution that may be stable in cases of linear loss which corresponds to stable background. This was first predicted for the cubic CGLE including the delayed response of the nonlinear refractive index [16] but later was extended to cases that, besides including the latter term, also include the other gradient terms [17]. Here, we report the existence of stable solitons for other cases of the cubic CGLE including gradient terms other than the delayed response of the nonlinear refractive index. The clue for the existence of these stable pulses was obtained by finding the equilibrium points of a system of four ordinary differential equations (ODEs) that resulted from a perturbation approach that used an ansatz similar to the exact chirped solutions of the cubic CGLE. Then, the amplitude and phase profiles of the actual solutions were obtained by solving a boundary value problem of another set of ODEs that resulted from the evolution equation by a similarity reduction, and their linear stability was investigated using the Evans function method. Finally, their existence was confirmed by direct integration of the evolution equation.

In Sec. II, we describe the methods, namely, the perturbation approach and the similarity reduction, as well as the strategy to study the solutions stability. There, we also present the main expressions for the parameters of the stationary perturbed solutions. In Sec. III, we investigate the solutions scenario for each isolated gradient term. The analysis is

*mines@fe.up.pt
†mfacao@ua.pt

done utilizing the three methods, the perturbation stationary solutions, the ODE solutions, and by fully integrating the evolution equation. Finally, we summarize the main results in Sec. IV.

II. EVOLUTION EQUATION AND METHODS

Consider the evolution equation

$$iq_Z - \frac{D}{2}q_{TT} + s|q|^2q = -iq + i\beta q_{TT} + i\epsilon|q|^2q + R(|q|^2)_Tq - iS(|q|^2q)_T, \quad (1)$$

where, in the optical context, q is the normalized envelope of the optical field and Z and T are the normalized propagation distance and retarded time, respectively. The parameters in this equation are all normalized versions of the actual parameters, namely, β for spectral filtering, ϵ for nonlinear gain, R for a delayed nonlinear response, and S for the dispersion of nonlinear effects. R and S are allowed to be complex, i.e., $R = R_r + iR_i$ and $S = S_r + iS_i$. In optics, the real part of R describes intrapulse Raman scattering which is responsible for soliton self frequency shift in conservative models [18–20] and has also been used in dissipative models [21]. The imaginary part of R models a delayed nonlinear gain. Also in optics, the real part of S corresponds to the dispersion of the Kerr effect and gives rise to the self-steepening effect [18–20,22] and the imaginary part corresponds to the dispersion of the nonlinear gain. The imaginary parts of R and S have not been added to the optical models, but would be useful to model resonant pulse propagation [9] and have been proposed in fluid dynamics [5]. The parameters D and s may only take the values ±1, $D = 1$ if the dispersion is normal and $D = -1$ if the dispersion is anomalous and $s = 1$ or $s = -1$ for positive or negative Kerr effect, respectively. The first term in the right hand side is responsible for linear loss. Note that we have applied a change of variables proposed in [17] which reduces the number of parameters.

A. Perturbation approach

In general, Eq. (1) does not exhibit closed form solutions. However, it allows solutions in the form of chirped solitons when $R = S = 0$ [9,15]. On the other hand, the left hand side of this equation is the well-known nonlinear Schrödinger equation (NLS), which possesses an infinite number of conserved quantities. The right hand side of the equation cancels the conservation of these quantities. However, expressions for their Z dependency may be deduced and those expressions are useful to find approximate solutions of the full equation (1) with small right-hand side. It should be noted that the success of this approach strongly depends on the right choice of the approximate profile. Recently, this approach was used in Eq. (1) by considering the soliton of the NLS, which approximated the infinite system (1) by a two-dimensional system [17]. Although some interesting results were found with this simple system, namely the prediction that the existence of stable solutions required R_r to be present, the phase profile of the considered perturbed soliton varies linearly with T and does not resemble the actual stationary pulse phase profile obtained by numerical methods. Therefore, in order to obtain a better agreement with the CGLE solitons, a more complex perturbed pulse must be considered. This can be done by allowing the amplitude and width to vary independently from each other, and also by including a chirp term in the phase. Traditionally, this chirp is added by considering a second-order expansion of the phase profile, which leads to a quadratic phase term [23–25]. However, in the case of CGLE solitons, that quadratic term would only represent a rough approximation of the actual soliton phase profile. Therefore, here we proceed by considering a pulse with a chirp that follows closely the CGLE chirped solitons:

$$q(T,Z) = A\,\mathrm{sech}(y)\exp(i\{\phi + b(T - T_0) + d\,\ln[\mathrm{sech}(y)]\}), \quad (2)$$

where $y = (T - T_0)/\omega$ and all the parameters A, T_0, ω, ϕ, b, and d are dependent on Z. The substitution of q in the evolution equation for the energy, momentum, and generalized momenta [23–25], which in this case are given by $Q = 2A^2\omega$, $P = -iQb$, $I_1 = QT_0$, $I_2 = \frac{\pi^2}{12}Q\omega^2$, and $I_3 = -iQd$, leads to the following set of coupled differential equations:

$$\frac{dQ}{dZ} = 2Q\left[-1 - \beta\left(b^2 + \frac{1}{3\omega^2}(1+d^2)\right) + \frac{Q}{3\omega}(\epsilon + S_ib)\right], \quad (3)$$

$$\frac{db}{dZ} = \frac{2}{3\omega^2}\left\{-2\beta b(1+d^2) + \frac{Q}{5\omega}[(2R_r + 3S_i) - 2(S_r - R_i)d + S_id^2]\right\}, \quad (4)$$

$$\frac{d\omega}{dZ} = \frac{2}{\pi^2}\left\{\frac{1}{\omega}[3Dd + 2\beta(2 - d^2)] - Q(\epsilon + S_ib)\right\}, \quad (5)$$

$$\frac{dd}{dZ} = \frac{2}{3\omega}\left\{\frac{1}{\omega}(D - \beta d)(1+d^2) + \frac{Q}{2}[s - (\epsilon + S_ib)d - S_rb]\right\},$$

$$\frac{dT_0}{dZ} = -Db + 2\beta bd + \frac{Q}{6\omega}[(3S_r - 2R_i) - S_id], \quad (6)$$

and

$$\frac{d\phi}{dZ} = \frac{D}{2}\left(b^2 + \frac{1+d^2}{3\omega^2}\right) + \frac{sQ}{3\omega} - \frac{S_rbQ}{3\omega} + b\frac{T_0}{dZ} + (1 - \ln 2)\frac{dd}{dZ} - \frac{d}{2\omega}\frac{d\omega}{dZ}$$

.

It is interesting to note that these six evolution equations involve all the coefficients in Eq. (1), unlike the perturbation equations based on the soliton of the NLS found in [17], which did not contain R_i and S_r. As it will be shown below, the presence of these two coefficients in these evolution equations is quite relevant, since they are also associated with the existence of stable stationary pulses.

Equations (3)–(6) do not depend on T_0 and ϕ. Furthermore, the evolution equations for T_0 and ϕ only depend on Q, b, ω, and d, implying that only Eqs. (3)–(6) need to be taken into account for the determination of the approximate pulse

solution given by Eq. (2). In the following, the stationary solutions of this four dimensional (4D) will be directly obtained as the roots of the right-hand sides of these four equations. In order to do so, we start by using Eqs. (5) and (4) to write

$$\frac{1}{\omega^2} = \frac{2(\epsilon + S_i b)A^2}{4\beta + 3Dd - 2\beta d^2}$$

and $b = EA^2$, where

$$E = \frac{2(R_r + R_i d - S_r d) + S_i(3 + d^2)}{5\beta(1 + d^2)}.$$

Moreover, A and d are found to satisfy

$$(-\beta E^2 + gS_i E)A^4 + g\epsilon A^2 - 1 = 0, \tag{7}$$

with

$$g = \frac{2(\beta + Dd - \beta d^2)}{4\beta + 3Dd - 2\beta d^2}$$

and

$$p(d) + [S_i(2D - 6\beta d - Dd^2) - S_r(4\beta + 3Dd - 2\beta d^2)]EA^2 = 0, \tag{8}$$

where we have defined

$$p(d) = -(D\epsilon + 2\beta s)d^2 - 3(2\epsilon\beta - Ds)d + 2(D\epsilon + 2\beta s).$$

Equations (7) and (8) are coupled to each other and, when solved, allow the determination of the stationary solution of (3)–(6) and thus an approximate solution to Eq. (1) given by (2). Furthermore, the linear stability properties of this solution can be investigated by computing the four eigenvalues of the (4×4) Jacobian matrix of the right-hand side of Eqs. (3)–(6) evaluated at the stationary solution. In order for a given stationary solution to be stable, the eigenvalues must be located in the half-plane with negative real part.

Also note that, as expected, for $R = S = 0$ this approximate solution coincides with the CGLE chirped soliton [9,15]. In this case, the previous equations lead to $b = 0$, $\omega^2 = \beta + Dd - \beta d^2$, and $A^2 = 1/g\epsilon$, with the chirp parameter d satisfying $p(d) = 0$, which indeed corresponds to the CGLE chirped soliton previously obtained. As pointed out in [9], these chirped solitons can only exist for one of the two solutions of the second order equation for d, namely for

$$d = \frac{3(sD - 2\beta\epsilon) + \sqrt{9(sD - 2\beta\epsilon)^2 + 8(D\epsilon + 2\beta s)^2}}{2(D\epsilon + 2\beta s)}. \tag{9}$$

Furthermore, for the equation written as in (1) which only admits linear loss, these solitons are only allowed when $\beta + Dd - \beta d^2 > 0$, that is, $\epsilon > \epsilon_s$ with $\epsilon_s = \frac{\beta(3\sqrt{1+4\beta^2}+Ds)}{4+18\beta^2}$, but are unstable in this region. However, it has been already shown that the presence of real R when $\beta > 0$ allows for the existence of another branch of solutions that are stable in a limited region of the (β, ϵ) plane [16,17].

B. Reduction to ODEs

The approach proposed in the previous subsection is valuable for finding stable solitary solutions of (1), as we shall see in the next section; however, an inspection of the actual stable solutions shows that, in some cases, the amplitude profiles are far from symmetric, and thus the assumed profile given by (2) is not a good estimate in those cases. As a consequence, the actual regions of existence of these solitons are also significantly different from the ones found within the perturbation approach.

Thus we have used another method to find the stationary solitary solutions, a numerical approach that is not as computationally expensive as the direct integration of Eq. (1). For that purpose, we assumed an ansatz of the form $q(Z, T) = F(t)e^{i\theta(t)+i\omega Z}$, with $t = T - vZ$ and real F and θ, that is inserted into the partial differential equation (PDE) (1) to obtain two ordinary differential equations, for F and $M = F^2\theta'$ [16,17], given by

$$\begin{aligned}
&\left(\frac{1}{2} + 2\beta^2\right)F'' + [2\beta v + D(2R_r + 3S_i)F^2 + 2\beta(2R_i - 3S_r)F^2]F' + (-2\beta + D\omega)F - Dv\frac{M}{F} - \left(\frac{1}{2} + 2\beta^2\right)\frac{M^2}{F^3} \\
&\quad + (-Ds + 2\beta\epsilon)F^3 + (DS_r + 2\beta S_i)FM = 0, \\
&\left(\frac{1}{2} + 2\beta^2\right)M' + [2\beta v + (DS_i - 2\beta S_r)F^2]M + [Dv + D(2R_i - 3S_r)F^2 - 2\beta(2R_r + 3S_i)F^2]FF' \\
&\quad + (-2\beta\omega - D)F^2 + (2\beta s + D\epsilon)F^4 = 0.
\end{aligned} \tag{10}$$

The solitary solutions should be the solutions of the above ODEs that obey $F \to 0$ for $t \to \pm\infty$. To find this kind of solution, we have used a shooting method for the PDE parameters that scanned the plane (β, ϵ) and $R_i \neq 0$ or $S_r \neq 0$. However, the solutions of the ODEs may be stable or unstable solutions of the PDE. Thus, to study their stability, we obtained the eigenvalues of the linear stability operator (see [17]) using the Evans function method [26,27].

III. RESULTS AND ANALYSIS

A. Existence and stability of approximated solutions

We now address the existence and stability of the stationary solutions of the 4D system obtained with the perturbation analysis in two different cases: when $S = 0$ and when $S \neq 0$.

1. S = 0

When $S = 0$, Eq. (8) becomes $p(d) = 0$, which implies that the chirp parameter d in the absence of nonlinear

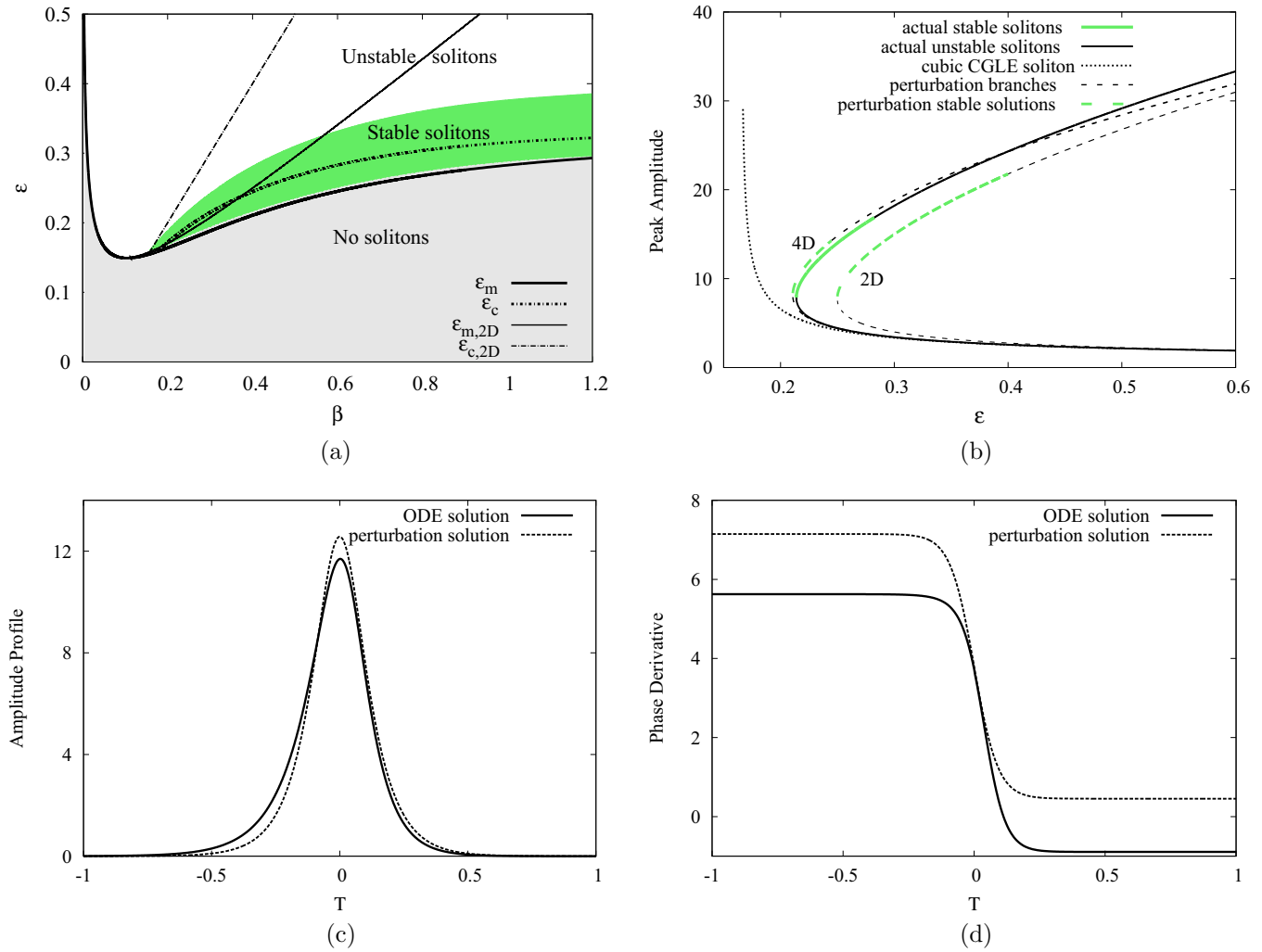

FIG. 1. Solutions for $R = 0.026$ and $S = 0$. Region of existence and stability (a): the lines associated with ϵ_m and ϵ_c correspond to the existence and stability boundaries, respectively, obtained with the perturbation approaches. Peak amplitude of the perturbation and ODE solutions and of the CGLE soliton as a function of ϵ for $\beta = 0.4$ (b). Comparison of (c) amplitude and (d) phase derivative profiles obtained with the perturbation approach and with the ODEs (10) for $\beta = 0.4$ and $\epsilon = 0.23$.

dispersion is the same as for the chirped solitons of the CGLE. In effect, even in the presence of complex R, the only root of $p(d)$ associated with real and positive values of A^2 and ω^2 is again the one satisfying Eq. (9). On the other hand, when E is not zero we find that

$$A^2 = \frac{g\epsilon \pm \sqrt{(g\epsilon)^2 - 4\beta E^2}}{2\beta E^2}.$$

Thus, if $\beta > 0$, two real and positive values of A^2 will be possible when $g\epsilon > 2|E|\sqrt{\beta}$, that is, when

$$\frac{\epsilon(\beta + Dd - \beta d^2)}{4\beta + 3Dd - 2\beta d^2} > \frac{2|R_r + R_i d|}{5(1+d^2)\sqrt{\beta}}.$$

This result implies that two different solutions might be allowed when $R_r + R_i d \neq 0$. In particular, this contradicts our previous result that R_r should always be present in order for two different solutions to be allowed [17]. Thus this perturbation analysis is saying that the terms associated with R_r or R_i are sufficient to allow another solution unless their effects cancel each other if $R_r + R_i d = 0$. Thus, regardless of the sign of $R_r + R_i d$, the previous condition defines for each value of β a minimum value of ϵ (ϵ_m). At ϵ_m the amplitude of the two solutions coincide and, below it, no solution is allowed.

As far as the stability is concerned, similar to what was shown in [16,17] for $R_r \neq 0$, in this 4D system with $S = 0$ and $R \neq 0$, we have found that the low-amplitude solution, which is very similar to the CGLE soliton, is always unstable, whereas the high amplitude one is stable in a limited region of the (β, ϵ) plane defined between ϵ_m and a critical value of ϵ (ϵ_c) that corresponds to the eigenvalues crossing the imaginary axis. It should be noted that, even though stationary solutions are allowed for any combination of coefficients D and s, we only found stable solutions when $Ds < 0$.

See the curves corresponding to the approximate solutions with R_r and R_i taken separately in Figs. 1 and 2.

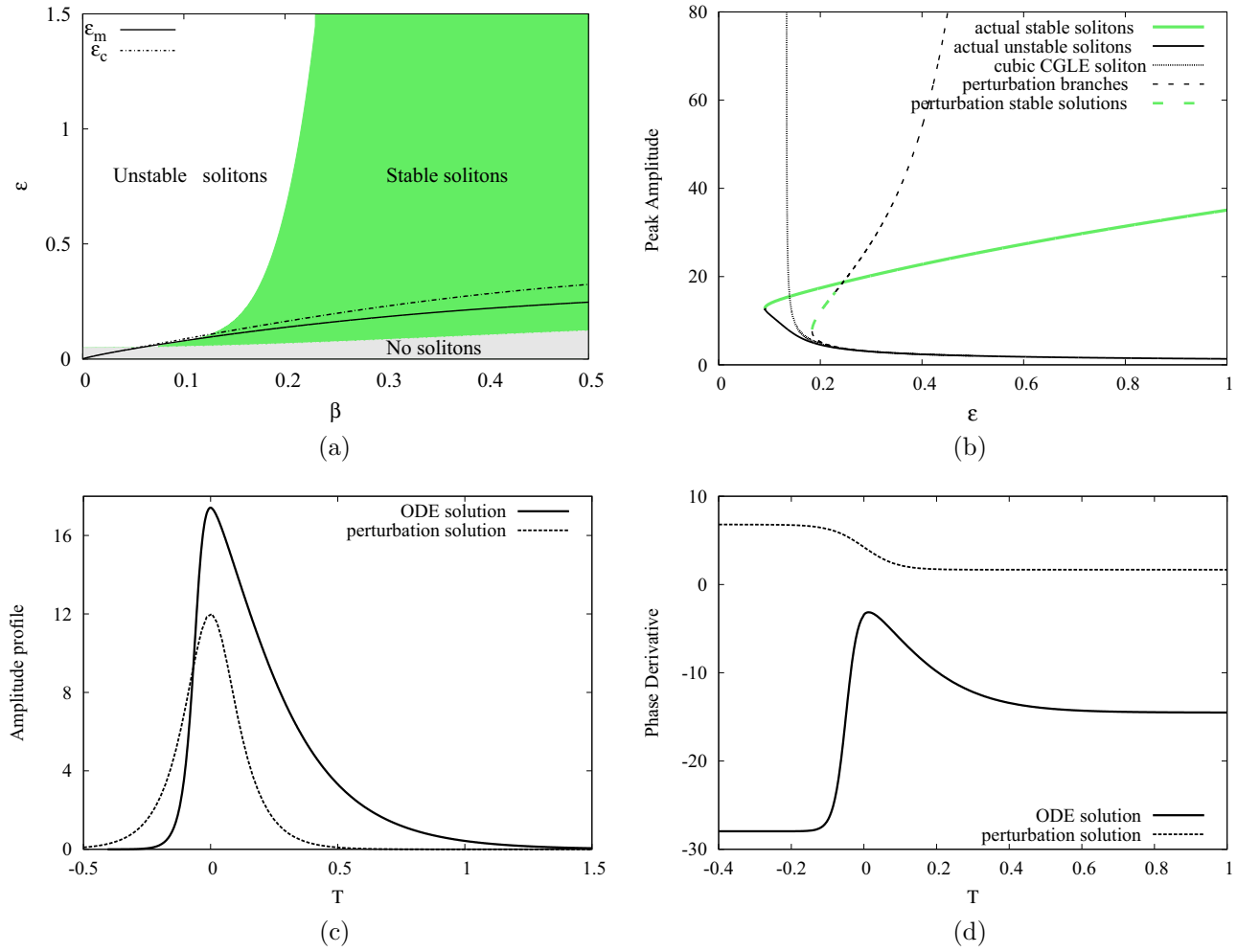

FIG. 2. Solutions for $R = 0.1i$ and $S = 0$. Region of existence and stability (a). Peak amplitude of the perturbation and ODE solutions and of the CGLE soliton as a function of ϵ for $\beta = 0.3$ (b). Comparison of (c) amplitude and (d) phase derivative profiles obtained with the perturbation approach and with the ODEs (10) for $\beta = 0.3$ and $\epsilon = 0.2$.

2. $S \neq 0$

When $S \neq 0$ we can use Eqs. (8) and (7) to write

$$A^2 = \frac{f(d)}{\beta E p(d) - 2(sS_i + \epsilon S_r)(\beta + Dd - \beta d^2)}$$

and

$$p(d)[2(sS_i + \epsilon S_r)(\beta + Dd - \beta d^2) - \beta E p(d)] - E f^2(d) = 0, \tag{11}$$

where, for simplicity, we have defined

$$f(d) = S_i(2D - 6\beta d - Dd^2) - S_r(4\beta + 3Dd - 2\beta d^2).$$

Equation (11) is a sixth-order polynomial equation for d. Note that, of all the roots of this polynomial, we are only interested in those corresponding to real and positive values of A^2 and ω^2.

The real and imaginary parts of S are associated with stationary solutions with different characteristics. When the effect of S_r is considered separately, we find a behavior similar to that of $S = 0$. Nevertheless, for lower values of ϵ, we now have one allowed solution, whereas with $S = 0$ we had none. This solution exists for $\epsilon > 0$ and is always unstable. Note that, for very small ϵ, that is, $\epsilon \simeq 0$, Eq. (11) predicts that $d \simeq 0$, which in turn implies that $A^2 \to \infty$. Furthermore, for larger ϵ two other solutions appear, increasing the number of allowed solutions to three. These two solutions have a behavior that closely resembles that of $S = 0$: the lower amplitude solution is similar to the CGLE soliton and is always unstable and the high amplitude one is stable in a limited ϵ region. See the curves corresponding to the perturbation approach in Fig. 3. It is also interesting to mention that, for low β, our perturbation approach predicts solutions besides the three already mentioned but, of all the five solutions we were able to obtain for low β [see Fig. 3(b)], only one was found to be stable in a limited ϵ region. Note that, as before, stable solutions were found only when $Ds < 0$.

The scenario with only S_i is quite different. Even though we found regions with one or with two allowed solutions, we were not able to find any stable solution.

B. Existence and stability of ODEs solutions

Let us first show the results for $R_r \neq 0$ that were already presented in our previous work [17]. Here we reproduce

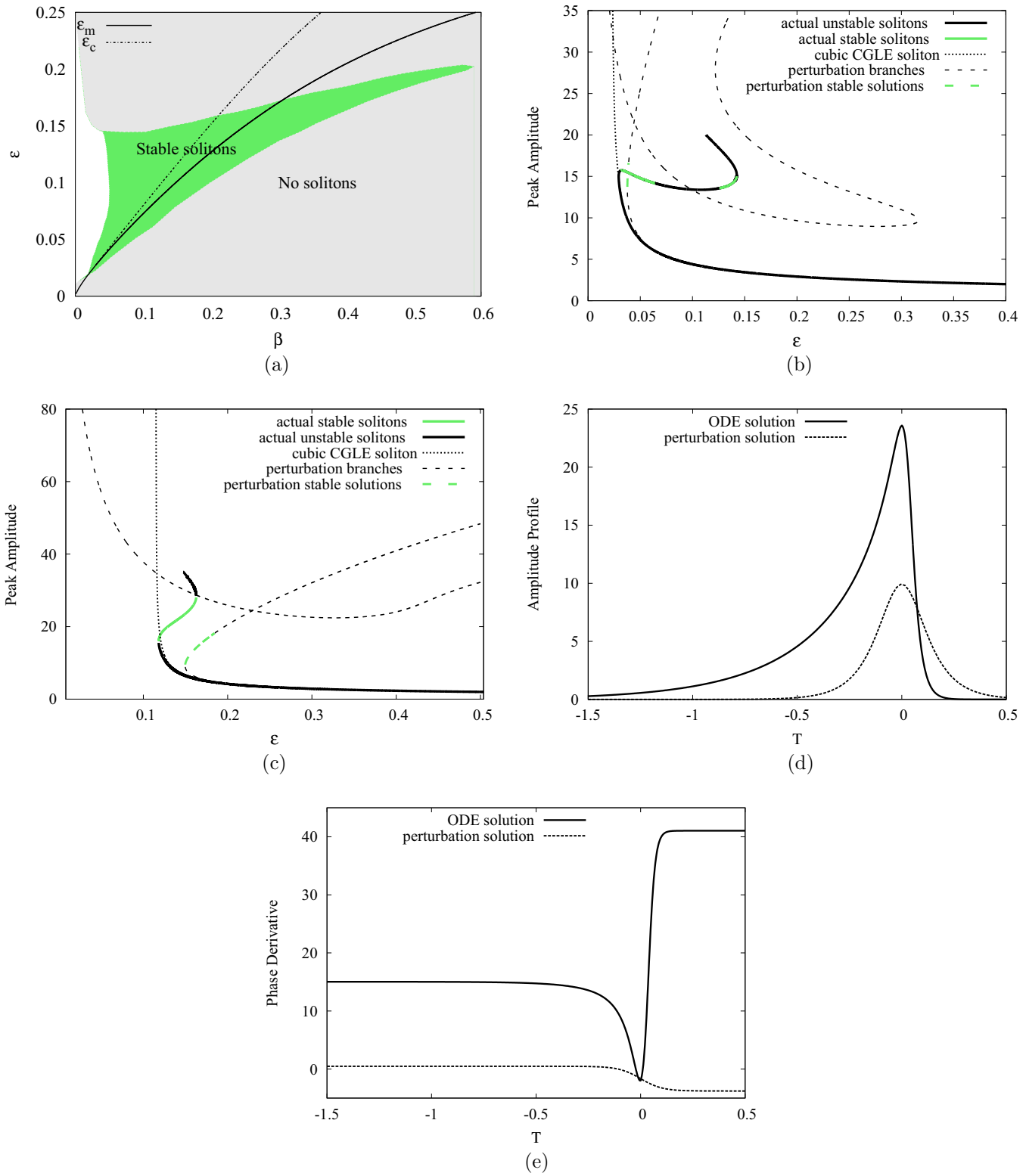

FIG. 3. Solutions for $R = 0$ and $S = 0.05$. Region of existence and stability (a). Peak amplitude of the perturbation and ODE solutions and of the CGLE soliton as a function of ϵ for (b) $\beta = 0.045$ and (c) $\beta = 0.25$. Comparison of (d) amplitude and (e) phase derivative profiles obtained with the perturbation approach and with the ODEs (10) for $\beta = 0.25$ and $\epsilon = 0.15$.

Fig. 2 of [17] for $R_r = 0.026$ [Fig. 1(a)], which shows the region of existence of stable solitons and that was obtained as indicated in Sec. II B. For comparison purposes, in this figure we have also represented the boundaries of the stability regions obtained with perturbation analysis using the chirpless NLS soliton (represented in the figure as "2D") and using the chirped soliton proposed here. Clearly, the 4D system considered allows a much better description of the stability region,

in particular, for higher values of ϵ. This better agreement of the 4D results can also be observed in Fig. 1(b), which depicts the peak amplitude of solutions of both branches for different values of ϵ. In Figs. 1(c) and 1(d) the amplitude and phase derivative profiles of the actual solutions and of the solutions obtained with the 4D perturbation system are shown for $\beta = 0.4$ and $\epsilon = 0.23$. Note that no solution is predicted by the 2D system for these β and ϵ values, since in this case $\epsilon_{m,2D}$ is approximately 0.25.

For $R_i \neq 0$, confirming the predictions of the perturbation approach used here, we have found two solutions above some minimal ϵ that may be distinguished by peak amplitude, as it is represented in Fig. 2(b) for $R_i = 0.1$ and $\beta = 0.3$. Note that the low amplitude solutions have peak amplitude very close to the peak amplitudes obtained by perturbation and also of the CGLE soliton; however, the same does not happen for the higher amplitude branch. In fact, the actual peak amplitudes are lower and increase slower with ϵ. Moreover, both branches exist for smaller β than it was predicted by the perturbation approach. We have not studied consistently the low amplitude solution but the few results that we have confirm that it is unstable. The higher amplitude solution is stable in certain regions of the existence parameter space as shown for $R_i = 0.1$ and $\beta = 0.3$ in Fig. 2(b) and in the (β, ϵ) plane also for $R_i = 0.1$ in Fig. 2(a). The existence and stability regions of the actual solitons are considerably different from the ones found by the perturbation analysis. The latter figure reveals that the curve for minimal ϵ for existence is almost independent of β and that the stable solutions exist from smaller ϵ and up to much larger ϵ than expected from the previous section. The reason for such disagreement should be in the discrepancy of the assumed profile in the perturbation approach and the actual solution profile as we may verify in Figs. 2(c) and 2(d) for the case $R = 0.1i$, $\beta = 0.3$, and $\epsilon = 0.2$. The peak amplitudes are considerably different; the actual amplitude profile is very asymmetric, with a steeper tail on the left. The actual phase derivative profile has very different right and left limits and also its structure at the peak location is considerably different from the tanh profile which characterizes the ansatz (2). Another property of the solutions is related with the sign of R_i, which is not relevant for existence and stability; symmetrical R_i produces solutions whose amplitude profiles are symmetrical in respect to T and that travel with opposite velocities but that exist and are stable in the same region of the parameter space. This effect of the sign of R_i is also predicted by the results of the 4D perturbation system considered here.

In the case of $S_r \neq 0$, we have found three branches of solutions as in Figs. 3(b) and 3(c). Two of them only exist above a certain ϵ and differ in peak amplitude. The lower peak amplitude branch extends to regions of large ϵ but the higher amplitude branch ceases to exist at certain ϵ at which the branch folds, in the lower ϵ direction, to another branch consisting of even higher peak amplitude pulses. In all the cases that we have studied, this latter branch ceases to exist at certain ϵ. Further studies are needed to understand this bifurcation. The only branch that has stable solutions is the one of intermediate peak amplitudes. As in the case of $R_i \neq 0$, the lower amplitude solutions obtained by the perturbation approach and using the ODEs are very similar regarding the peak amplitude. However, the actual high amplitude solutions have higher peak amplitude than predicted and, as noted above, do not extend to regions of large ϵ but cease to exist at the point where the other branch starts. In Fig. 3(a), we show the region of existence and stability of the intermediate amplitude branch for $S_r = 0.05$. In the same figure, we show the lines for ϵ_m and ϵ_c obtained with the perturbation approach also for its intermediate peak amplitude branch. From this perspective, the two results show a significant disagreement as well. This disagreement can also be justified by the fact that the profile assumed in the perturbation is considerably different from the actual one, as we show in Figs. 3(d) and 3(e). For the parameters here considered, there was no evidence of any other branch. The results concerning existence and stability are again not dependent on the sign of S_r but, as in the case of $R_i \neq 0$, the change of the sign of S_r transforms the amplitude profile in the symmetrical one with respect to T and also changes the sign of the velocity.

It should also be noted that, even though discrepancies were found between the actual solutions and the ones associated with the 4D perturbation system when R_i and S_r are the only gradient terms, mainly in the phase derivative profile and stability region, the 4D system is able to predict relevant characteristics of the solutions exhibited by Eq. (1). In particular, unlike the simpler 2D perturbation system which has only one unstable solution branch in these cases [17], the 4D system presented here is able to anticipate the existence of more branches of solutions, with one of them being stable in a given parameter region. Finally, let us mention that, similar to what was obtained using either perturbation method, we were not able to find any stable solution from the numerical integration of (10) when S_i is the only nonzero gradient term. Furthermore, although we have considered here each of the gradient terms separately, stable solutions are allowed for combinations of these terms, even if those combinations also include S_i. Examples of the solutions when different terms are added to R_r can be found in [17].

C. Full integration of the PDE

In order to confirm the existence of the stable solutions presented in Sec. II, including their amplitude and phase derivative profiles and parameter regions, we have integrated (1) directly using unchirped sech profiles as inputs. After a distance of adjustment, the amplitude and phase profiles are in good agreement with the ones obtained using the ODEs. To verify the parameter regions where the stable solutions do exist, we have done the integration referred to above for randomly chosen pairs of (β, ϵ) in each stability region of Figs. 2(a) and 3(a). Apart from some discrepancies for (β, ϵ) at the boundaries of those regions that we attribute to numerical inaccuracies of the Evans method or to a limited basin of attraction of the stable solution, the PDE integration confirmed the regions of stable propagation. In Fig. 4, we show the evolution of $15\,\mathrm{sech}\,(15T)$ and $25\,\mathrm{sech}\,(25T)$ to stable pulses for $\beta = 0.3$, $\epsilon = 0.2$, $R = 0.1i$, and $S = 0$ and $\beta = 0.25$, $\epsilon = 0.15$, $R = 0$, and $S = 0.05$, respectively.

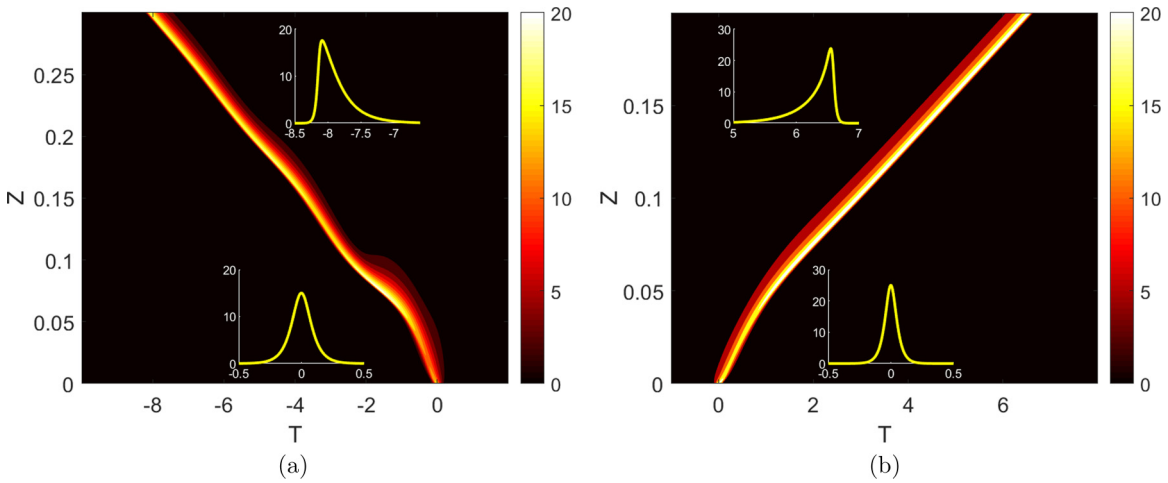

FIG. 4. Evolution to stable pulses of (a) $15\,\mathrm{sech}\,(15T)$ for $\beta = 0.3$, $\epsilon = 0.2$, $R = 0.1i$, and $S = 0$ and of (b) $25\,\mathrm{sech}\,(25T)$ for $\beta = 0.25$, $\epsilon = 0.15$, $R = 0$, and $S = 0.05$. The insets show the input amplitude profile (bottom) and the output amplitude profile (top).

IV. CONCLUSIONS

Following a perturbation approach that uses six modified conservation laws of the NLS and a chirped soliton of the cubic CGLE, we were able to predict the existence of branches of solutions, stable in certain regions, for two generalizations of the cubic CGLE, one including a term responsible for a delayed nonlinear gain and another contemplating dispersion of the nonlinear refractive index (an effect that is also known as self-steepening). In previous publications, it was assumed that the existence of stable solitons requires that the delayed nonlinear refractive index (also known as intrapulse Raman scattering) was nonzero. However, here we proved that these perturbation results were valuable and that, in fact, the cubic CGLE admits stable solitons whenever one of those two terms is nonzero, such that they do not require the presence of intrapulse Raman scattering. The amplitude profiles of these solitons are very asymmetric and their phase derivatives have a considerable structure in the peak location. The parameter region of those stable solitons is large in both cases but especially for nonzero delayed nonlinear gain. These results enlarge the known conditions for stable pulse propagation in systems modeled by generalizations of the CGLE which include the gradient terms considered. Furthermore, these results may be useful in other areas of physics where the CGLE is applicable.

ACKNOWLEDGMENTS

This work is financed by National Funds through the Portuguese funding agency, FCT—Fundação para a Ciência e a Tecnologia—within Projects No. UID/EEA/50014/2019 and No. UID/CTM/50025/2019.

[1] N. Akhmediev and A. Ankiewicz, *Dissipative Solitons*, Lecture Notes in Physics (Springer, Berlin, 2005).
[2] N. Akhmediev and A. Ankiewicz, *Dissipative Solitons: From Optics to Biology and Medicine*, Lecture Notes in Physics (Springer, Berlin, 2008).
[3] O. Thual and S. Fauve, J. Phys. France **49**, 1829 (1988).
[4] W. van Saarloos and P. C. Hohenberg, Phys. Rev. Lett. **64**, 749 (1990).
[5] R. J. Deissler and H. R. Brand, Phys. Lett. A **146**, 252 (1990).
[6] H. Haus, J. Fujimoto, and E. Ippen, J. Opt. Soc. Am. B **8**, 2068 (1991).
[7] M. Matsumoto, H. Ikeda, T. Uda, and A. Hasegawa, J. Lightwave Technol. **13**, 658 (1995).
[8] P. Grelu and N. Akhmediev, Nat. Photon. **6**, 84 (2012).
[9] M. Facão, S. Rodrigues, and M. I. Carvalho, Phys. Rev. A **91**, 013828 (2015).
[10] J. M. Soto-Crespo, M. Grapinet, P. Grelu, and N. Akhmediev, Phys. Rev. E **70**, 066612 (2004).
[11] L. Duan, X. Liu, D. Mao, L. Wang, and G. Wang, Opt. Express **20**, 265 (2012).
[12] L. M. Zhao, A. C. Bartnik, Q. Q. Tai, and F. W. Wise, Opt. Lett. **38**, 1942 (2013).
[13] R. J. Deissler and H. R. Brand, Phys. Rev. Lett. **72**, 478 (1994).
[14] R. J. Deissler and H. R. Brand, Phys. Rev. Lett. **81**, 3856 (1998).
[15] N. N. Akhmediev, V. V. Afanasjev, and J. M. Soto-Crespo, Phys. Rev. E **53**, 1190 (1996).
[16] M. Facão and M. I. Carvalho, Phys. Rev. E **92**, 022922 (2015).
[17] M. Facão and M. I. Carvalho, Phys. Rev. E **96**, 042220 (2017).
[18] G. Agrawal, *Nonlinear Fiber Optics*, 5th ed. (Academic Press, Boston, 2012).
[19] L. Bergé, J. J. Rasmussen, and J. Wyller, J. Phys. A: Math. Gen. **29**, 3581 (1996).
[20] J. S. Hesthaven, J. J. Rasmussen, L. Bergé, and J. Wyller, J. Phys. A: Math. Gen. **30**, 8207 (1997).
[21] M. Karpov, H. Guo, A. Kordts, V. Brasch, M. H. P. Pfeiffer, M. Zervas, M. Geiselmann, and T. J. Kippenberg, Phys. Rev. Lett. **116**, 103902 (2016).

[22] M. R. E. Lamont, Y. Okawachi, and A. L. Gaeta, Opt. Lett. **38**, 3478 (2013).
[23] A. I. Maimistov, JETP **77**, 727 (1993).
[24] E. Tsoy and N. Akhmediev, Phys. Lett. A **343**, 417 (2005).
[25] E. N. Tsoy, A. Ankiewicz, and N. Akhmediev, Phys. Rev. E **73**, 036621 (2006).
[26] J. Evans, Indiana Univ. Math. J. **24**, 1169 (1975).
[27] J. Alexander, R. Gardner, and C. Jones, J. Reine Angew. Math. **410**, 167 (1990).